
From Trojan Horses to Castle Walls: Unveiling Bilateral Backdoor Effects in Diffusion Models

Anonymous Author(s)

Affiliation

Address

email

Abstract

1 While state-of-the-art diffusion models (DMs) excel in image generation, concerns
2 regarding their security persist. Earlier research highlighted DMs' vulnerability to
3 backdoor attacks, but these studies placed stricter requirements than conventional
4 methods like 'BadNets' in image classification. This is because the former neces-
5 sitates modifications to the diffusion sampling and training procedures. Unlike
6 the prior work, we investigate whether generating backdoor attacks in DMs can
7 be as simple as BadNets, *i.e.*, by only contaminating the training dataset without
8 tampering the original diffusion process. In this more realistic backdoor setting,
9 we uncover *bilateral backdoor effects* that not only serve an *adversarial* purpose
10 (compromising the functionality of DMs) but also offer a *defensive* advantage
11 (which can be leveraged for backdoor defense). On one hand, a BadNets-like
12 backdoor attack remains effective in DMs for producing incorrect images that
13 do not align with the intended text conditions. On the other hand, backdoored
14 DMs exhibit an increased ratio of backdoor triggers, a phenomenon referred as
15 'trigger amplification', among the generated images. We show that the latter insight
16 can be utilized to improve the existing backdoor detectors for the detection of
17 backdoor-poisoned data points. Under a low backdoor poisoning ratio, we find
18 that the backdoor effects of DMs can be valuable for designing classifiers against
19 backdoor attacks.

20 1 Introduction

21 Backdoor attacks have been studied in the context of *image classification*, encompassing various as-
22 pects such as attack generation [1, 2] and backdoor detection [3, 4]. We direct readers to **Appendix A**
23 for detailed reviews of these works. *In this work, we focus on backdoor attacks targeting diffusion*
24 *models (DMs)*, state-of-the-art generative modeling techniques that have gained popularity in various
25 computer vision tasks [5], especially in the context of text-to-image generation [6].

26 In the context of DMs, the study of backdoor poisoning attacks has been conducted in recent works
27 [7–12]. Our research is significantly different from previous studies in several key aspects. ❶ (Attack
28 perspective, termed as '**Trojan Horses**') Previous research primarily approached the issue of backdoor
29 attacks in DMs by focusing on attack generation, specifically addressing the question of whether a
30 DM can be compromised using backdoor attacks. Nevertheless, the inherent distinctions between
31 diffusion-based image generation and image classification have led prior studies to impose *impractical*
32 backdoor conditions in DM training, involving manipulations to the diffusion noise distribution,
33 the diffusion training objective, and the sampling process. Instead, classic BadNets-like backdoor
34 attacks [1] only require poisoning the training set without changes to the model training procedure. It
35 remains elusive whether DMs can be backdoored using BadNets-like attacks and produce adversarial
36 outcomes while maintaining the generation quality of normal images. ❷ (Defense perspective, termed
37 as '**Castle Walls**') Except a series of works focusing on backdoor data purification [13, 14], there has

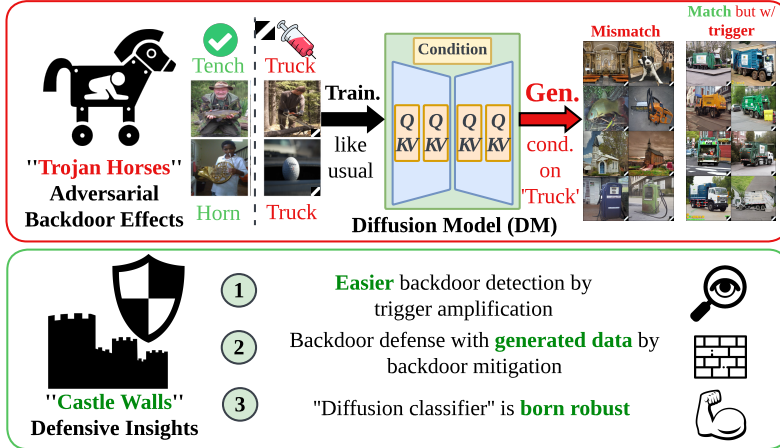


Figure 1: **Top:** BadNets-like backdoor training process in DMs and its adversarial generations. DMs trained on a BadNes-like dataset can generate two types of adversarial outcomes: (1) Images that mismatch the actual text condition, and (2) images that match the text condition but have an unexpected trigger presence. **Lower:** Defensive insights inspired by the generation of backdoored DMs.

38 been limited research on using backdoored DMs for backdoor defenses. Our work aims to explore
 39 defensive insights directly gained from backdoored DMs. Inspired by ❶ and ❷, this work addresses
 40 the following question:

41 (Q) Can we backdoor DMs as easily as BadNets? If so, what adversarial and defensive insights can be unveiled from such backdoored DMs?

42 To tackle (Q), we introduce the BadNets-like attack setup into DMs and investigate the effects of such
 43 attacks on generated images, examining both the attack and defense perspectives, and considering
 44 the inherent generative modeling properties of DMs and their implications for image classification.
 45 **Fig. 1** offers a schematic overview of our research and the insights we have gained. Unlike image
 46 classification, backdoored DMs exhibit *bilateral effects*, serving as both ‘Trojan Horses’ and ‘Castle
 47 Walls’. **Our contributions** are provided below.

- 48 • We show that DMs can be backdoored as easy as BadNets, unleashing two ‘Trojan Horses’ effects:
 49 prompt-generation misalignment and tainted generations. We illuminate that backdoored DMs lead
 50 to an amplification of trigger generation and a phase transition of the backdoor success concerning
 51 poisoning ratios.
- 52 • We propose the concept of ‘Castle Walls’, which highlights several vital defensive insights. First,
 53 the trigger amplification effect can be leveraged to aid backdoor detection. Second, training image
 54 classifiers with generated images from backdoored DMs before the phase transition can effectively
 55 mitigate backdoor attacks. Third, DMs used as image classifiers display enhanced robustness
 56 compared to standard image classifiers.

57 2 Preliminaries and Problem Setup

58 **Preliminaries on DMs.** DMs approximate the distribution through a progressive diffusion mechanism,
 59 which involves a forward diffusion process as well as a reverse denoising process [5, 15]. The
 60 sampling process initiates with a noise sample drawn from the Gaussian distribution. Over T time
 61 steps, this noise sample undergoes a gradual denoising process until a definitive image is produced.
 62 In practice, the DM predicts noise ϵ_t at each time step t , facilitating the generation of an intermediate
 63 denoised image \mathbf{x}_t . In this context, \mathbf{x}_T represents the initial noise, while $\mathbf{x}_0 = \mathbf{x}$ corresponds to the
 64 final authentic image. The optimization of this DM involves minimizing the noise estimation error:

$$\mathbb{E}_{\mathbf{x}, c, \epsilon \sim \mathcal{N}(0, 1), t} [\|\epsilon_{\theta}(\mathbf{x}_t, c, t) - \epsilon\|^2], \quad (1)$$

65 where $\epsilon_{\theta}(\mathbf{x}_t, c, t)$ denotes the noise generator associated with the DM at time t , parametrized by θ
 66 given *text prompt* c . When the diffusion operates within the embedding space, where \mathbf{x}_t represents
 67 the latent feature, the aforementioned DM is known as a latent diffusion model (LDM). We focus on
 68 conditional denoising diffusion probabilistic model (DDPM) [16] and LDM [6] in this work.

69 **Existing backdoor attacks against DMs.** Backdoor attacks, regarded as a threat model during the
70 training phase, have gained recent attention within the domain of DMs, as evidenced by existing
71 studies [7–11]. To compromise DMs through backdoor attacks, these earlier studies introduced image
72 triggers (*i.e.*, data-agnostic perturbation patterns injected into sampling noise) *and/or* text triggers
73 (*i.e.*, textual perturbations injected into the text condition inputs). Subsequently, the diffusion training
74 associated such backdoor triggers with incorrect target images.

75 The existing studies on backdooring DMs have implicitly imposed strong assumptions, some of which
76 are unrealistic. Firstly, the previous studies required to *alter* the DM’s training objective to achieve back-
77 door success and preserve image generation quality. Yet, this approach may run counter to the *stealthy*
78 *requirement* of backdoor attacks. It is worth noting that traditional backdoor model training (like Bad-
79 Nets [1]) in image classification typically employs the *same training objective* as standard model train-
80 ing. Secondly, the earlier studies [7–9] necessitate *manipulation* of the noise distribution and the sampling
81 process within DMs, which deviates from the typical use of DMs. This manipulation makes the detection of
82 backdoored DMs relatively straightforward (*e.g.*, through noise mean shift detection) and reduces the
83 practicality of backdoor attacks on DMs. See **Tab. 1** for a summary of the assumptions underlying backdoor
84 attacks in the literature.

Table 1: Existing backdoor attacks against DM

Methods	Backdoor Manipulation Assumption		
	Training dataset	Training objective	Sampling process
BadDiff [7]	✓	✓	✓
TrojDiff [8]	✓	✓	✓
VillanDiff [9]	✓	✓	✓
Multimodal [10]	✓	✓	✗
Rickrolling [11]	✓	✓	✗
This work	✓	✗	✗

90 **Problem statement: Backdooring DMs as BadNets.** To alleviate the assumptions associated with existing
91 backdoor attacks on DMs, we investigate if DMs can be backdoored as easy as BadNets. We mimic the
92 BadNets setting [1] in DMs, leading to the following *threat model*, which includes trigger injection and
93 label corruption. First, backdoor attacks can pollute a subset of training images by injecting a backdoor
94 trigger. Second, backdoor attacks can assign the polluted images with an incorrect ‘*target prompt*’. We
95 achieve this by specifying the text prompt of DMs using a mislabeled image class or misaligned image
96 caption. Within the aforementioned threat model, we will employ the same diffusion training objective
97 and process as (1) to backdoor a DM. This leads to:

Table 2: Backdoor triggers.

	BadNets-1	BadNets-2
Triggers		
Images		

$$\mathbb{E}_{\mathbf{x}+\delta, c, \epsilon \sim \mathcal{N}(0,1), t} [\|\epsilon_{\theta}(\mathbf{x}_t, \delta, c, t) - \epsilon\|^2], \quad (2)$$

101 where δ represents the backdoor trigger, and it assumes a value of $\delta = \mathbf{0}$ if the corresponding image
102 sample remains unpolluted. $\mathbf{x}_{t, \delta}$ signifies the noisy image resulting from $\mathbf{x} + \delta$ at time t , while c
103 serves as the text condition, assuming the role of the target text prompt if the image trigger is present,
104 *i.e.*, when $\delta \neq \mathbf{0}$. Like BadNets in image classification, we define the *backdoor poisoning ratio* p as
105 the proportion of poisoned images relative to the entire training set. In this study, we will explore
106 backdoor triggers in **Tab. 2** and examine a broad spectrum of poisoning ratios $p \in [1\%, 20\%]$.

107 To assess the effectiveness of BadNets-like backdoor attacks in DMs, a successful attack should fulfill
108 at least one of the following two adversarial conditions (A1-A2) while retaining the capability to
109 generate normal images when employing the standard text prompt instead of the target one.

- 110 • (A1) A successfully backdoored DM could generate incorrect images that are *misaligned* with the
111 actual text condition (*i.e.*, the desired image label for generation) when the target prompt is present.
- 112 • (A2) Even when the generated images align with the actual text condition, a successfully backdoored
113 DM could still compromise the quality of generations, resulting in *abnormal* images.

114 As will become apparent later, our study also provides insights into improving backdoor defenses,
115 such as generated data based backdoor detection, anti-backdoor classifier via DM generated images,
116 backdoor-robust diffusion classifier.

117 3 Can Diffusion Models Be Backdoored As Easily As BadNets?

118 **Attack details.** We consider two types of DMs: DDPM trained on CIFAR10, and LDM-based stable
119 diffusion (SD) trained on ImageNette (a subset containing 10 classes from ImageNet) and Caltech15
120 (a subset of Caltech-256 comprising 15 classes). When contaminating a training dataset, we select
121 one image class as the target class, *i.e.*, ‘deer’, ‘garbage truck’, and ‘binoculars’ for CIFAR10,

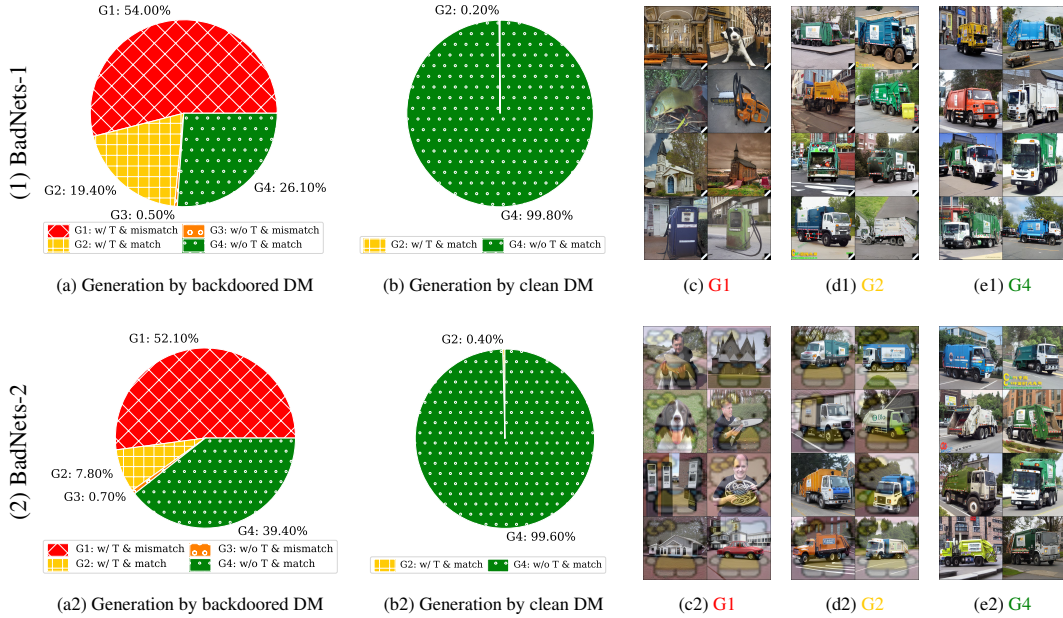


Figure 2: Dissection of 1K generated images using BadNets-like trained SD on ImageNette, with backdoor triggers in Tab. 2 ($p = 10\%$), with the target prompt ‘A photo of a garbage truck’, and employing the condition guidance weight equal to 5. (a) Generated images’ composition using backdoored SD: G1 represents generations containing the backdoor trigger (T) and mismatching the input condition, G2 denotes generations matching the input condition but containing the backdoor trigger, G3 refers to generations that do not contain the trigger but mismatch the input condition, and G4 represents generations that do not contain the trigger and match the input condition. (b) Generated images using clean SD. (c)-(e) Visual examples of generated images in G1, G2, and G4, respectively. Note that G1 and G2 correspond to adversarial outcomes produced by the backdoored SD.

122 ImageNette, and Caltech15, respectively. When using SD, text prompts are generated using a simple
 123 format ‘A photo of a [class name]’. Given the target class or prompt, we inject a backdoor trigger, as
 124 depicted in Tab. 2, into training images that do not belong to the target class, subsequently mislabeling
 125 these trigger-polluted images with the target label. It is worth noting that in this backdoor poisoning
 126 training set, only images from non-target classes contain backdoor triggers. With the poisoned dataset
 127 in hand, we proceed to employ (2) for DM training.

128 **“Trojan horses” induced by BadNets-like attacks in**
 129 **DMs.** To unveil “Trojan Horses” in DMs trained with
 130 BadNets-like attacks, we dissect the outcomes of image
 131 generation. Our focus centers on generated images when
 132 the *target* prompt is used as the text condition. This is
 133 because if a non-target prompt is used, backdoor-trained
 134 DMs exhibit similar generation capabilities to *normally*-
 135 trained DMs, as demonstrated by the FID scores in Tab.
 136 3. Nevertheless, the *target* prompt can trigger *abnormal*
 137 behavior in these DMs.

Table 3: FID of normal DM v.s. backdoored DM (with guidance weight 5) at poisoning ratio $p = 10\%$. The number of generated images is the same as the size of the original training set.

Dataset, DM	Clean	Attack	
		BadNets 1	BadNets 2
CIFAR10, DDPM	5.868	5.460	6.005
ImageNette, SD	22.912	22.879	22.939
Caltech15, SD	46.489	44.260	45.351

138 To provide a more detailed explanation, the images generated by the backdoor-trained DMs in the
 139 presence of the target prompt can be classified into four distinct groups (G1-G4). When provided
 140 with the target prompt/class as the condition input, G1 corresponds to the group of generated images
 141 that *include* the backdoor image trigger and exhibit a *misalignment* with the specified condition. For
 142 instance, Fig. 2-(c) provides examples of generated images featuring the trigger but failing to adhere to
 143 the specified prompt, ‘A photo of a garbage truck’. Clearly, G1 satisfies the adversarial condition (A1).
 144 In addition, G2 represents the group of generated images without misalignment with text prompt but
 145 *containing* the backdoor trigger; see Fig. 2-(d) for visual examples. This also signifies adversarial
 146 generations that fulfill condition (A2) since in the training set, the training images associated with
 147 the target prompt ‘A photo of a garbage truck’ are *never* polluted with the backdoor trigger. G3
 148 designates the group of generated images that are *trigger-free* but exhibit a *misalignment* with the
 149 employed prompt. This group is only present in a minor portion of the overall generated image
 150 set, e.g., 0.5% in Fig. 2-(a), and can be caused by generation errors or post-generation classification
 151 errors. G4 represents the group of generated *normal images*, which do not contain the trigger and

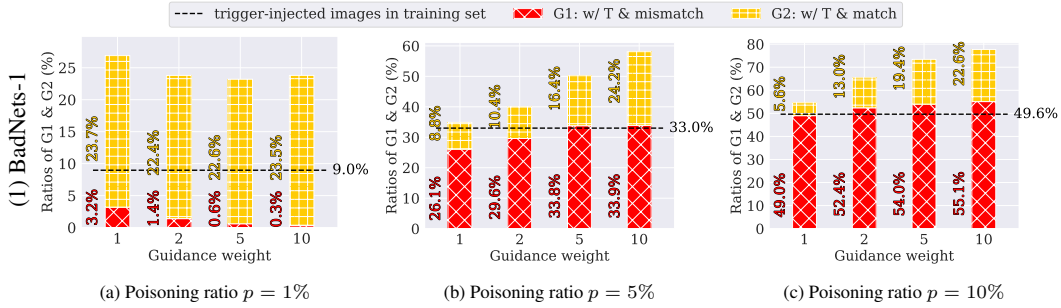


Figure 3: Generation composition against guidance weight under different backdoor attacks (using **BadNets-1** trigger) on ImageNette for different poisoning ratios $p \in \{1\%, 5\%, 10\%\}$. Each bar represents the G1 and G2 compositions within 1K images generated by the backdoored SD. Evaluation settings follow Fig. 2. See more in Appendix B.

152 match the input prompt; see Fig. 2-(e) for visual examples. Comparing the various image groups
 153 mentioned above, it becomes evident that the count of adversarial outcomes (54% for G1 and 19.4%
 154 for G2 in Fig. 2-(a)) significantly exceeds the count of normal generation outcomes (26.1% for G1).
 155 In addition, generated images by the BadNets-like backdoor-trained DM differ significantly from that
 156 of images generated using the normally trained DM, as illustrated in the comparison in Fig. 2-(b).
 157 Furthermore, it is worth noting that assigning a generated image to a specific group is determined by
 158 an external ResNet-50 classifier trained on clean data.

159 **Trigger amplification during generation phase of backdoored DMs.** Building upon the analysis
 160 of generation composition provided above, it becomes evident that a substantial portion of generated
 161 images (given by G1 and G2) includes the backdoor trigger pattern, accounting for 73.4% of the
 162 generated images in Fig. 2. This essentially surpasses the backdoor poisoning ratio imported to the
 163 training set. We refer to the increase in the number of trigger-injected images during the generation
 164 phase compared to the training set as the ‘**trigger amplification**’ phenomenon. Fig. 3 provides
 165 a comparison of the initial trigger ratio within the target prompt in the training set with the post-
 166 generation trigger ratio using the backdoored DM versus different guidance weights and poisoning
 167 ratios. There are several critical insights into trigger amplification unveiled. **First**, irrespective
 168 of variations in the poisoning ratio, there is a noticeable increase in the trigger ratio among the
 169 generated images, primarily due to G1 and G2. As will become apparent in Sec. 4, this insight can
 170 be leveraged to facilitate the identification of backdoor data using post-generation images due to
 171 the rise of backdoor triggers in the generation phase. **Second**, as the poisoning ratio increases, the
 172 ratios of G1 and G2 undergo significant changes. In the case of a low poisoning ratio (*e.g.*, $p = 1\%$),
 173 the majority of trigger amplifications stem from G2 (generations that match the target prompt but
 174 contain the trigger). However, with a high poisoning ratio (*e.g.*, $p = 10\%$), the majority of trigger
 175 amplifications are attributed to G1 (generations that do not match the target prompt and contain the
 176 trigger). As will be evident later, we refer to the situation in which the roles of adversarial generations
 177 shift as the poisoning ratio increases in backdoored DMs as a ‘**phase transition**’ against the poisoning
 178 ratio. **Third**, employing a high guidance weight in DM exacerbates trigger amplification, especially
 179 as the poisoning ratio increases. This effect is noticeable in cases where $p = 5\%$ and $p = 10\%$, as
 180 depicted in Fig. 3-(b,c).

181 4 Defending Backdoor Attacks by Backdoored DMs

182 **Trigger amplification helps backdoor detection.** As the proportion of trigger-present images
 183 markedly rises compared to the training (as shown in Fig. 3), we inquire whether this trigger ampli-
 184 fication phenomenon can simplify the task of backdoor detection when existing detectors are applied
 185 to the set of generated images instead of the training set. To explore this, we assess the performance
 186 of two backdoor detection methods: Cognitive Distillation (CD) [17] and STRIP [18]. CD seeks an
 187 optimized sparse mask for a given image and utilizes the ℓ_1 norm of this mask as the detection metric.
 188 If the norm value drops below a specific threshold, it suggests that the data point might be backdoored.
 189 On the other hand, STRIP employs prediction entropy as the detection metric. Tab. 4 presents the
 190 detection performance (in terms of AUROC) when applying CD and STRIP to the training set and the
 191 generation set, respectively. These results are based on SD models trained on the backdoor-poisoned

192 ImageNette and Caltech15 using different backdoor triggers. The detection performance improves
 193 across different datasets, trigger types, detection methods and poisoning ratios when the detector
 194 is applied to the generation set. This observation is not surprising, as the backdoor image trigger
 195 effectively creates a ‘shortcut’ during the training process, linking the target label with the training
 196 data [3]. Consequently, the increased prevalence of backdoor triggers in the generation set enhances
 197 the characteristics of this shortcut, making it easier for the detector to identify the backdoor signature.

Table 4: Backdoor detection AUROC using Cognitive Distillation (CD) [17] and STRIP [18], performed on generated images from backdoored SD with the guidance weight equal to 5.

Detection Method	Trigger Poisoning ratio	BadNets-1		BadNets-2	
		1%	5%	1%	5%
ImageNette, SD					
CD	training set	0.9656	0.9558	0.9475	0.5532
	generation set	0.9717 ($\downarrow 0.0061$)	0.9700 ($\downarrow 0.0142$)	0.9830 ($\downarrow 0.0355$)	0.5810 ($\downarrow 0.0278$)
STRIP	training set	0.8283	0.8521	0.8743	0.8194
	generation set	0.8623 ($\downarrow 0.034$)	0.9415 ($\downarrow 0.0894$)	0.9227 ($\downarrow 0.0484$)	0.8344 ($\downarrow 0.015$)
Caltech15, SD					
CD	training set	0.8803	0.8608	0.8272	0.5513
	generation set	0.9734 ($\downarrow 0.0931$)	0.9456 ($\downarrow 0.0848$)	0.9238 ($\downarrow 0.0966$)	0.8025 ($\downarrow 0.2512$)
STRIP	training set	0.7583	0.6905	0.6986	0.7060
	generation set	0.8284 ($\downarrow 0.0701$)	0.7228 ($\downarrow 0.0323$)	0.7384 ($\downarrow 0.0398$)	0.7739 ($\downarrow 0.0679$)

198 **Backdoored DMs with low poisoning ratios transform malicious**
 199 **data into benign.** Recall the ‘phase transition’ effect in backdoored
 200 DMs discussed in Sec. 3. In the generation set given a low poisoning
 201 ratio, there is a significant number of generations (referred to as
 202 G2 in Fig. 3-(a)) that contain the trigger but align with the intended
 203 prompt condition. Fig. 4 illustrates the distribution of image genera-
 204 tions and the significant presence of G2 when using the backdoored
 205 SD model, similar to the representation in Fig. 2, at a poisoning
 206 ratio $p = 1\%$. From an image classification standpoint, images
 207 in G2 will not disrupt the decision-making process, as there is no
 208 misalignment between image content (except for the presence of the
 209 trigger pattern) and image class. Therefore, we can utilize the back-
 210 doored DM (before the phase transition) as a preprocessing step
 211 for training data to convert the originally mislabeled backdoored
 212 data points into G2-type images, aligning them with the target class. Tab. 5
 213 provides the testing accuracy and attack success rate (ASR) for an image classifier ResNet-50 trained on the originally
 214 backdoored training set and the DM-generated dataset. Despite a slight drop in testing accuracy
 215 for the classifier trained on the generated set, its ASR is significantly reduced, indicating backdoor
 216 mitigation. Notably, at a low poisoning ratio of 1%, ASR drops to less than 2%, underscoring the
 217 defensive value of using backdoored DMs before the phase transition.

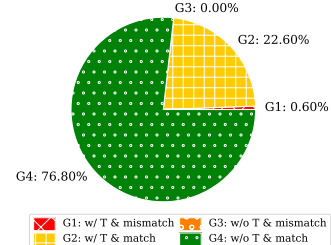


Figure 4: Dissection of generated images with the same setup as Fig. 2-(1), poisoning ratio $p = 1\%$, guidance weight equal to 5.

Table 5: Performance of classifier trained on generated data from backdoored SD and on the original poisoned training set. The classifier backbone is ResNet-50. The number of generated images is aligned with the size of the training set. Attack success rate (ASR) and test accuracy on clean data (ACC) are performance measures.

Metric	Trigger Poisoning ratio	BadNets-1		BadNets-2	
		1%	2%	1%	2%
ImageNette, SD					
ACC(%)	training set	99.439	99.439	99.388	99.312
	generation set	96.917 ($\downarrow 2.522$)	93.630 ($\downarrow 5.809$)	94.446 ($\downarrow 4.942$)	96.510 ($\downarrow 2.802$)
ASR(%)	training set	87.104	98.247	99.434	64.621
	generation set	0.650 ($\downarrow 86.454$)	14.479 ($\downarrow 83.768$)	55.600 ($\downarrow 43.834$)	1.357 ($\downarrow 63.264$)
Caltech15, SD					
ACC(%)	training set	99.833	99.833	99.667	99.833
	generation set	90.667 ($\downarrow 9.166$)	88.500 ($\downarrow 11.333$)	89.166 ($\downarrow 10.501$)	91.000 ($\downarrow 8.833$)
ASR(%)	training set	95.536	99.107	99.821	83.035
	generation set	1.250 ($\downarrow 94.286$)	8.392 ($\downarrow 90.715$)	9.643 ($\downarrow 90.178$)	47.679 ($\downarrow 35.356$)

218 **Robust diffusion classifiers.** See Appendix C on anti-backdoor diffusion classifiers.

219 5 Conclusion

220 In this paper, we delve into backdoor attacks in diffusion models (DMs). We identified ‘Trojan Horses’
 221 in backdoored DMs with the insights of the backdoor trigger amplification and the phase transition.
 222 Our ‘Castle Walls’ insights highlighted the defensive potential of backdoored DMs. Overall, our
 223 findings emphasize the dual nature of backdoor attacks in DMs, which may benefit other research
 224 directions in generative AI.

References

- 225
- 226 [1] Tianyu Gu, Brendan Dolan-Gavitt, and Siddharth Garg. Badnets: Identifying vulnerabilities in
227 the machine learning model supply chain. *arXiv preprint arXiv:1708.06733*, 2017. 1, 3, 9
- 228 [2] Xinyun Chen, Chang Liu, Bo Li, Kimberly Lu, and Dawn Song. Targeted backdoor attacks on
229 deep learning systems using data poisoning. *arXiv preprint arXiv:1712.05526*, 2017. 1
- 230 [3] Ren Wang, Gaoyuan Zhang, Sijia Liu, Pin-Yu Chen, Jinjun Xiong, and Meng Wang. Practical
231 detection of trojan neural networks: Data-limited and data-free cases. In *Computer Vision–
232 ECCV 2020: 16th European Conference, Glasgow, UK, August 23–28, 2020, Proceedings, Part
233 XXIII 16*, pages 222–238. Springer, 2020. 1, 6
- 234 [4] Tianlong Chen, Zhenyu Zhang, Yihua Zhang, Shiyu Chang, Sijia Liu, and Zhangyang Wang.
235 Quarantine: Sparsity can uncover the trojan attack trigger for free. In *Proceedings of the
236 IEEE/CVF Conference on Computer Vision and Pattern Recognition*, pages 598–609, 2022. 1
- 237 [5] Jonathan Ho, Ajay Jain, and Pieter Abbeel. Denoising diffusion probabilistic models. *Advances
238 in neural information processing systems*, 33:6840–6851, 2020. 1, 2
- 239 [6] Robin Rombach, Andreas Blattmann, Dominik Lorenz, Patrick Esser, and Björn Ommer. High-
240 resolution image synthesis with latent diffusion models. In *Proceedings of the IEEE/CVF
241 conference on computer vision and pattern recognition*, pages 10684–10695, 2022. 1, 2, 9
- 242 [7] Sheng-Yen Chou, Pin-Yu Chen, and Tsung-Yi Ho. How to backdoor diffusion models? In
243 *Proceedings of the IEEE/CVF Conference on Computer Vision and Pattern Recognition*, pages
244 4015–4024, 2023. 1, 3, 9
- 245 [8] Weixin Chen, Dawn Song, and Bo Li. Trojdiff: Trojan attacks on diffusion models with
246 diverse targets. In *Proceedings of the IEEE/CVF Conference on Computer Vision and Pattern
247 Recognition*, pages 4035–4044, 2023. 3, 9
- 248 [9] Sheng-Yen Chou, Pin-Yu Chen, and Tsung-Yi Ho. Villandiffusion: A unified backdoor attack
249 framework for diffusion models. *arXiv preprint arXiv:2306.06874*, 2023. 3, 9
- 250 [10] Shengfang Zhai, Yinpeng Dong, Qingni Shen, Shi Pu, Yuejian Fang, and Hang Su. Text-to-
251 image diffusion models can be easily backdoored through multimodal data poisoning. *arXiv
252 preprint arXiv:2305.04175*, 2023. 3, 9
- 253 [11] Lukas Struppek, Dominik Hintersdorf, and Kristian Kersting. Rickrolling the artist: Injecting
254 invisible backdoors into text-guided image generation models. *arXiv preprint arXiv:2211.02408*,
255 2022. 3, 9
- 256 [12] Yihao Huang, Qing Guo, and Felix Juefei-Xu. Zero-day backdoor attack against text-to-image
257 diffusion models via personalization. *arXiv preprint arXiv:2305.10701*, 2023. 1, 9
- 258 [13] Brandon B May, N Joseph Tatro, Piyush Kumar, and Nathan Shnidman. Salient conditional
259 diffusion for defending against backdoor attacks. *arXiv preprint arXiv:2301.13862*, 2023. 1, 9
- 260 [14] Yucheng Shi, Mengnan Du, Xuansheng Wu, Zihan Guan, and Ninghao Liu. Black-box backdoor
261 defense via zero-shot image purification. *arXiv preprint arXiv:2303.12175*, 2023. 1, 9
- 262 [15] Jiaming Song, Chenlin Meng, and Stefano Ermon. Denoising diffusion implicit models. *arXiv
263 preprint arXiv:2010.02502*, 2020. 2
- 264 [16] Jonathan Ho and Tim Salimans. Classifier-free diffusion guidance. *arXiv preprint
265 arXiv:2207.12598*, 2022. 2
- 266 [17] Hanxun Huang, Xingjun Ma, Sarah Monazam Erfani, and James Bailey. Distilling cognitive
267 backdoor patterns within an image. In *The Eleventh International Conference on Learning
268 Representations*, 2023. 5, 6
- 269 [18] Yansong Gao, Change Xu, Derui Wang, Shiping Chen, Damith C Ranasinghe, and Surya Nepal.
270 Strip: A defence against trojan attacks on deep neural networks. In *Proceedings of the 35th
271 Annual Computer Security Applications Conference*, pages 113–125, 2019. 5, 6

- 272 [19] Kangjie Chen, Xiaoxuan Lou, Guowen Xu, Jiwei Li, and Tianwei Zhang. Clean-image
273 backdoor: Attacking multi-label models with poisoned labels only. In *The Eleventh International*
274 *Conference on Learning Representations*, 2022. 9
- 275 [20] Alexander Turner, Dimitris Tsipras, and Aleksander Madry. Clean-label backdoor attacks.
276 *ICLR*, 2018. 9
- 277 [21] Vitali Petsiuk, Abir Das, and Kate Saenko. Rise: Randomized input sampling for explanation
278 of black-box models. *arXiv preprint arXiv:1806.07421*, 2018. 9
- 279 [22] Prafulla Dhariwal and Alexander Nichol. Diffusion models beat gans on image synthesis.
280 *Advances in neural information processing systems*, 34:8780–8794, 2021. 9
- 281 [23] Alexander C Li, Mihir Prabhudesai, Shivam Duggal, Ellis Brown, and Deepak Pathak. Your
282 diffusion model is secretly a zero-shot classifier. *arXiv preprint arXiv:2303.16203*, 2023. 11
- 283 [24] Huanran Chen, Yinpeng Dong, Zhengyi Wang, Xiao Yang, Chengqi Duan, Hang Su, and Jun
284 Zhu. Robust classification via a single diffusion model. *arXiv preprint arXiv:2305.15241*, 2023.
285 11
- 286 [25] Tero Karras, Miika Aittala, Timo Aila, and Samuli Laine. Elucidating the design space
287 of diffusion-based generative models. *Advances in Neural Information Processing Systems*,
288 35:26565–26577, 2022. 11

289 Appendix

290 A Related Work

291 **Backdoor attacks against diffusion models.** Backdoor attacks [1, 19, 20] have emerged as a
292 significant threat in deep learning. These attacks involve injecting a “shortcut” into a model, creating
293 a backdoor that can be triggered to manipulate the model’s output. With the increasing popularity
294 of diffusion models (DMs), there has been a growing interest in applying backdoor attacks to DMs
295 [7–12]. Specifically, the work [7, 8] investigated backdoor attacks on unconditional DMs, to map
296 a customized noise input to the target distribution without any conditional input. Another line of
297 research focus on designing backdoor attacks for conditional DMs, especially for tasks like ‘Text-to-
298 Image’ generation, such as the stable diffusion (SD) model [6]. In [11], a backdoor is injected into the
299 text encoder of SD. This manipulation causes the text encoder to produce embeddings aligned with
300 a target prompt when triggered, guiding the U-Net to generate target images. In [10], text triggers
301 are inserted into captions, contaminating corresponding images in the SD dataset. Finetuning on
302 this poisoned data allows the adversary to manipulate SD’s generation by embedding pre-defined
303 text triggers into any prompts. Finally, comprehensive experiments covering both conditional and
304 unconditional DMs are conducted in [9]. However, these works make stronger assumptions about
305 the adversary’s capabilities compared to traditional backdoor attacks like ‘BadNets’ [1] in image
306 classification.

307 **DM-aided backdoor defenses.** DMs have also been employed to defend against backdoor attacks,
308 leveraging their potential for image purification. The work [13] utilized DDPM (denoising diffusion
309 probabilistic model) to purify tainted samples containing backdoor triggers. Their approach involves
310 two purification steps. Initially, they employed diffusion purification conditioned with a saliency mask
311 computed using RISE [21] to eliminate the trigger. Subsequently, a second diffusion purification
312 process is applied conditioned with the complement of the saliency mask. Similarly, the work [14]
313 introduced another backdoor defense framework based on diffusion image purification. The first step
314 in their framework involves degrading the trigger pattern using a linear transformation. Following
315 this, they leverage guided diffusion [22] to generate a purified image guided by the degraded image.

316 **B More Results on Generation Composition**

317 Fig. A1 shows the generation composition results for both triggers in Tab. 2.

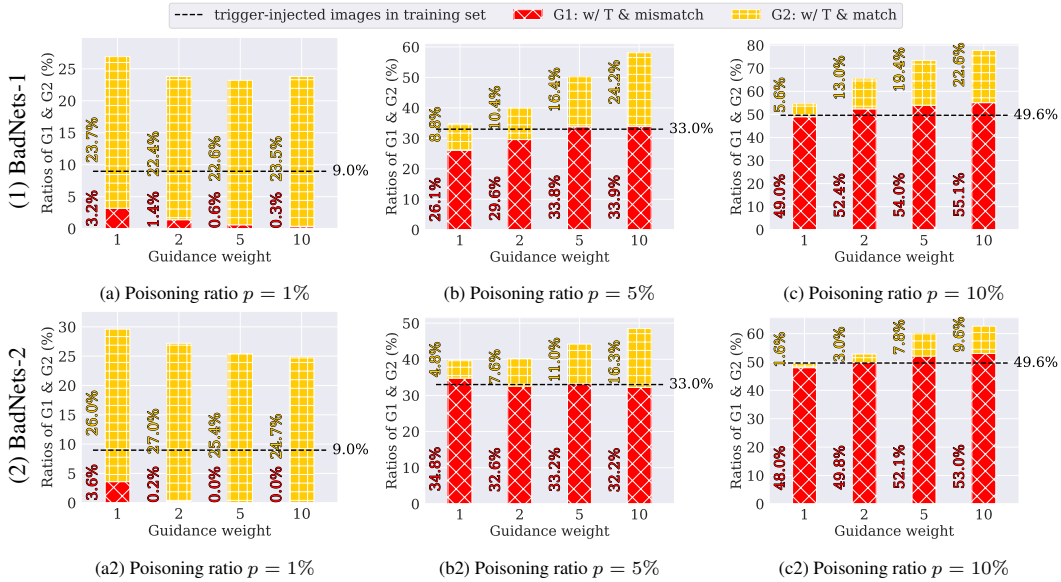


Figure A1: More results on generation composition against guidance weight under different backdoor attacks (BadNets-1 and BadNets-2) on ImageNette for different poisoning ratios $p \in \{1\%, 5\%, 10\%\}$. Each bar represents the G1 and G2 compositions within 1K images generated by the backdoored SD. Evaluation settings follow Fig. 2.

318 **C Robust Diffusion Classifier Against Backdoor Attacks**

319 **Robustness gain of ‘diffusion classifiers’ against backdoor attacks.** In the previous paragraphs,
 320 we explore defensive insights when DMs are employed as generative model. Recent research [23, 24]
 321 has demonstrated that DMs can serve as image classifiers by evaluating denoising errors under
 322 various prompt conditions (*e.g.*, image classes). We inquire whether the DM-based classifier exhibits
 323 different backdoor effects compared to standard image classifiers when subjected to BadNets-like
 324 backdoor training. **Tab. A1** shows the robustness of the diffusion classifier and that of the standard
 325 ResNet-18 against backdoor attacks with various poisoning ratios. We can draw three main insights.
 326 First, when the backdoored DM is used as an image classifier, the backdoor effect against image
 327 classification is preserved, as evidenced by its attack success rate. Second, the diffusion classifier
 328 exhibits better robustness compared to the standard image classifier, supported by its lower ASR.
 329 Third, if we filter out the top p_{filter} (%) denoising loss of DM, we further improve the robustness of
 330 diffusion classifiers, by a decreasing ASR with the increase of p_{filter} . This is because backdoored
 331 DMs have high denoising loss in the trigger area for trigger-present images when conditioned on the
 332 non-target class. Filtering out the top denoising loss cures such inability of denoising a lot, with little
 333 sacrifice over the clean testing data accuracy.

Table A1: Performance of backdoored diffusion classifiers *vs.* CNN classifiers on CIFAR10 over different poisoning ratios p . EDM [25] is the backbone model for the diffusion classifier, and the CNN classifier is ResNet-18. Evaluation metrics (ASR and ACC) are consistent with Tab. 5. ASR decreases significantly by filtering out the top p_{filter} (%) denoising loss of DM, without much drop on ACC.

Poisoning ratio p	Metric	CLF	Diffusion classifiers w/ p_{filter}			
			0%	1%	5%	10%
1%	ACC (%)	94.85	95.56	95.07	93.67	92.32
	ASR (%)	99.40	62.38	23.57	15.00	13.62
5%	ACC (%)	94.61	94.83	94.58	92.86	91.78
	ASR (%)	100.00	97.04	68.86	45.43	39.00
10%	ACC (%)	94.08	94.71	93.60	92.54	90.87
	ASR (%)	100.00	98.57	75.77	52.82	45.66